

CFD ANALYSIS OF VAPOR CHAMBER WITH MICRO PILLARS AS HEAT SPREADER
FOR HIGH POWER ELECTRONIC DEVICES

By

YASIR AZIZ MODAK

Presented to the Faculty of the Graduate School of
The University of Texas at Arlington in Partial Fulfillment
of the Requirements
for the Degree of

MASTER OF SCIENCE IN MECHANICAL ENGINEERING
THE UNIVERSITY OF TEXAS AT ARLINGTON

MAY 2016

Copyright © by Yasir Aziz Modak 2016

All Rights Reserved



Acknowledgements

I would like to take this opportunity to thank my thesis guide Dr. Dereje Agonafer, who was a source of inspiration to me throughout my work. I would also like to thank him for his relentless guidance in my research studies and to help me explore my hidden potentials.

I would also like to thank Dr. Haji-Sheikh and Dr. Miguel Amaya for being on my thesis committee. A special thanks to Ms. Sally Thompson and Ms. Debi Barton for their tremendous help throughout my stay at UT Arlington.

Finally, I would like to dedicate my thesis to my parents who made me what I am today. I am very grateful to my father Mr. Aziz Modak and mother Mrs. Nasrin Modak for their colossal faith in me. I could have never got this far without their support and love. I am blessed to have a brother Mr Aamir Modak who always encouraged me to widen my horizons of thinking and backed me.

April 14, 2016

Abstract

CFD ANALYSIS OF VAPOR CHAMBER WITH MICRO PILLARS AS HEAT SPREADER FOR HIGH POWER ELECTRONIC DEVICES

Yasir Aziz Modak, MS

The University of Texas at Arlington, 2016

Supervising Professor: Dereje Agonafer

The recent trend in electronic industry shows that there is large power dissipation from the electronic devices and at the same time their sizes are getting smaller. This large power dissipation takes place in the form of releasing heat energy. It is observed that heat dissipation from the electronic devices is high and source size is small. The high device temperatures result in decreased reliability and increased failure rates. This difficulty can be addressed by controlling the temperatures at the source of heat generation. In chip scale package chip is the major source of heat generation. Thus our priority is to keep the junction temperature as low as possible at given thermal design power. This is usually achieved by using finned heat sinks at the top of the package.

A heat sink is designed to maximize its surface area in contact with the cooling medium surrounding it, such as the air. The amount of heat transferred by the heat sink to the air depends on the surface area of heat sink and air flowing over it. The surface area of heat sink is dictated by parameters such as weight, noise, availability of space, vibrations, surroundings, cost etc. Spreading resistance occurs due to small size source attached at the base of large heat sink.

The research provides an aggressive approach to control or eliminate spreading resistance by developing a vapor chamber heat sink with micro pillars. The two phase heat transfer provided by the vapor chambers deliver a higher performance and alleviate

the thermal spreading resistance. The research focuses on the CFD analysis of vapor chamber with micro pillars as better heat spreader. The extensive parametric study suggests that this technology provides efficient cooling options for microelectronics. The proposed CFD model offers 14% less thermal resistance than that of conventional copper heat spreaders.

Table of Contents

Acknowledgements	iii
Abstract	iv
List of Illustrations	ix
List of Tables	x
Chapter 1 Introduction to Electronic Packaging	1
1.1 Electronic Packaging	1
1.2 Levels of Electronic Packaging	1
1.3 Thermal Management in Electronic Packaging	3
1.4 Trends in Electronic Cooling Solutions	3
Chapter 2 Two Phase Cooling Solutions: Heat Pipe and Vapor Chamber	4
2.1 Introduction to Heat Pipe and Vapor Chamber	4
2.2 Types of Wick Structures	6
2.2.1 Sintered Wick	7
2.2.2 Mesh or Grooved Wick	7
2.2.3 Screen Wick	7
2.3 Effective Thermal Conductivity of Wick Structure	8
2.4 Types of Working Fluid	10
2.5 Effective Thermal Conductivity of Vapor Space	11
Chapter 3 Computational Fluid Dynamics (CFD) Study	13
3.1 Introduction	13

3.2 Methodology.....	13
Chapter 4 Computational Fluid Dynamics (CFD) Modeling of Vapor Chamber with Micro Pillars.....	16
4.1 Model Setup in ANSYS-Icepak.....	18
4.2 Part Modelling in ANSYS-Icepak.....	18
4.2.1 Cabinet.....	18
4.2.2 Block.....	18
4.2.3 Plate.....	19
4.2.4 Source.....	19
4.3 Analysis Setup.....	20
4.3.1 Generating Mesh.....	20
4.3.2 Basic Parameters.....	20
4.3.3 Solution Settings.....	21
4.4 Analysis Results.....	21
4.4.1 Contour Plots: Plane Cut Temperature.....	21
4.4.2 Temperature Contours.....	22
4.5 Intel 6 th Generation Core i7 Chipset.....	24
4.5.1 Thermal Profile.....	24
Chapter 5 Parametric Study of Vapor Chamber with Micro Pillars.....	27
5.1 Effect of changes in heat spreader width.....	27
5.2 Effect of effective thermal conductivity of wick and vapor space.....	28
5.3 Effect of convective heat transfer coefficient of heat sink base.....	31
5.4 Effect of heat sink base size.....	33
Chapter 6 Conclusion.....	35
6.1 Summary.....	35

6.2 Conclusion.....	36
References.....	37
Biographical Information.....	38

List of Illustrations

Figure 1-1 Levels of electronic packaging	2
Figure 2-1 Working of a heat pipe.....	4
Figure 2-2 Working of a vapor chamber	5
Figure 2-3 Types of wick structures	6
Figure 4-1 CFD model of vapor chamber with micro pillars.....	16
Figure 4-2 Plane cut temperature for vapor chamber with micro pillars model.....	21
Figure 4-3 Plane cut temperature for copper spreader model.....	22
Figure 4-4 Top surface temperature distribution of chip surface	22
Figure 4-5 Top surface temperature distribution of heat spreader	23
Figure 4-6 Thermal profile of intel 6th gen core i7 TTV.....	25
Figure 4-7 Thermal profile vapor chamber model and copper spreader model.....	25
Figure 5-1 Effect of heat spreader width on junction and case temperature on vapor chamber with micro pillars model and copper spreader model.....	28
Figure 5-2 Effect of wick thermal conductivity on junction temperature of vapor chamber with micro pillars model.....	29
Figure 5-3 Effect of vapor thermal conductivity on junction temperature of vapor chamber with micro pillars model.....	30
Figure 5-4 Effect of convective heat transfer coefficient on junction temperature.....	31
Figure 5-5 Effect of convective heat transfer coefficient on case temperature.....	32
Figure 5-6 Effect of heat sink base size on junction temperature.....	33
Figure 5-7 Effect of heat sink base size on case temperature.....	34

List of Tables

Table 2-1 Properties of different wick structures	8
Table 2-2 Values of effective wick thermal conductivity	9
Table 2-3 Types of working fluids used in two phase devices.....	10
Table 4-1 Material properties and dimensions of different parts of the vapor chamber with micro pillars model (baseline study).....	17

Chapter 1

Introduction to Electronic Packaging

1.1 Electronic Packaging

The electronic packaging is a multi-disciplinary field of electronics, materials, and mechanical engineering which can be defined as a science of encasing electronic components or electronic assemblies so as to protect them from environmental hazards such as moisture, dust etc., human mishandling and most importantly effective heat dissipation from the electronics. The electronic packaging basically suffices following factors; mechanical requirements, electrical requirements, and thermal requirements. The mechanical requirements include, providing proper housing/ encapsulation to electronic package, preventing adverse effects of environment and protecting from physical damage. The electrical requirements include unrestricted and undisturbed flow of electrical signals to electronic circuits with no lag and high reliability. It performs the function of signal distribution and power distribution to the package. The thermal requirements are one of the most important factor of electronic packaging. The reliability of package is affected by excessive temperature rises, thus packaging serves as efficient path for the heat dissipation from the die in case of chip level cooling. Therefore, keeping the junction temperature within operating limits and avoiding overheating of the package. The packaging is basically done at three levels, chip level, board level, and system level.

1.2 Levels of Electronic Packaging

To satisfy the wide array of requirements of electronic components the packaging of these devices is carried out in three levels. This is done in order to perform each task single handedly and provide efficient packaging solutions to all parts of the package. The figure 1.1 which is taken from Lau's book [1], schematically represents different levels of

electronic packaging and gives an idea of hierarchy in these levels. They can be elaborated as follows:

- 1) First Level Package (Chip Module): This level consists of providing interconnection directly to the integrated circuit chip. It provides mounting of IC on to the chip carrier thus protecting it from environment.
- 2) Second Level Package (PCB): This level consists of one or more first level packages mounted on Printed Circuit Board (PCB) which are generally interconnected with the aid of lead solder.
- 3) Third Level Package (Motherboard): This level consists of rigid mounting of PCB's, peripheral electronic components and providing electrical connection through wires.

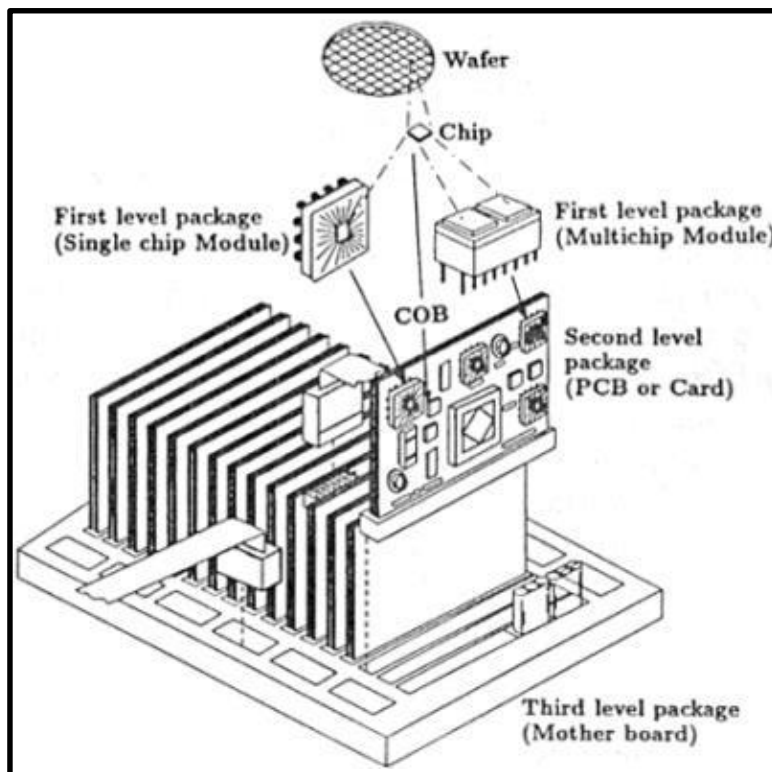


Figure 1-1 Levels of Electronic Packaging

Packaging of electronic circuits is the science and specialty of building up interconnection and a suitable working environment for dominating electrical circuits to process or store data.

1.3 Thermal Management in Electronic Packaging

The thermal management of electronics is a significant issue due to ever increasing power densities and miniaturization of microsystem electronics. Thus extracting heat from these systems had become a very important task which needs to be addressed at earliest. The reliability of the component is directly affected by rise in temperature and hence efficient cooling solutions should be provided to keep the temperatures within permissible range. The cooling is usually done by air cooling, high performance liquid cooling which is water or oil immersion cooling and by using two phase cooling techniques. The cooling techniques adopted are dictated by various parameters such as weight, design, size, operating temperatures, reliability, cost etc.

1.4 Trends in Electronic Cooling Solutions

The CPU power consumption is expected to increase with each new generation of computers whereas the geometries are shrinking. This has resulted in increasing power densities of chip, high thermal hot spots and large variation of temperature in the dies. These problems cannot be addressed to full potential due to limited surface area for heat dissipation. Heat sinks serve a vital role in alleviating hot spots and reducing thermal spreading but still fail to solve the purpose. We can observe tremendous high fluxes at particular locations and hot spots in spite of using heat sinks. However, it has been observed by that provision of two phase cooling at the bottom of heat sinks reduces the hot spots drastically.

Chapter 2

Two Phase Cooling Solutions: Heat Pipes and Vapor Chambers

2.1 Introduction to Heat Pipe and Vapor Chamber

The two phase cooling solutions provides high thermal performance results in electronic cooling. The heat pipes and vapor chamber as most widely used two phase cooling devices. Both transfer heat through phase change of liquid into vapor and back from vapor into liquid. In each of the design the liquid is passively pumped from the condenser side to the evaporator side by capillary action of wick structure. They provide high reliability with no noise or moving parts.

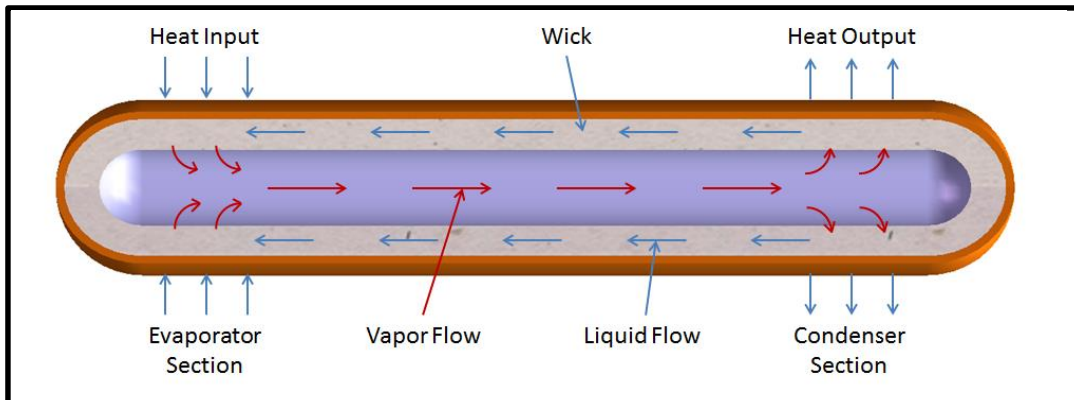


Figure 2-1 Working of a Heat Pipe

The heat pipe is a vacuum sealed tube with prescribed amount of working fluid at its bottom. It has wick structure inside the tube i.e. inner lining of tube is wick. When heat is applied at the bottom side i.e. at the evaporator section the fluid vaporizes and moves towards the cooler region i.e. condenser section (Heat Sink) due the pressure created by the temperature difference between two sections. This vaporized fluid gives up its latent heat of vaporization and condenses into liquid. This condensed liquid is brought back to the evaporator section by the capillary action of the wick structure.

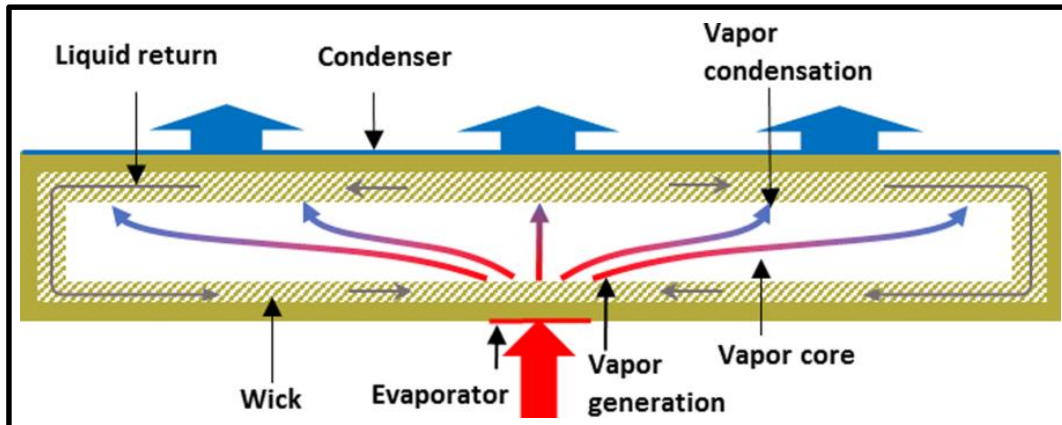


Figure: 2-2 Working of a Vapor Chamber

A vapor chamber is vacuum sealed rectangular heat pipe with wick alignment inside the inner walls of the vapor chamber [2]. The wick is saturated with the working fluid. When heat is applied at the bottom of vapor chamber i.e. at lower copper wall (Evaporator Section) the fluid in the wick structure vaporizes. This fluid rushes to fill vacuum and comes in contact with the cooler region. It gives away its latent heat of vaporization at the condenser section and condenses back into liquid which is again brought back to evaporator section by the capillary action of the wick.

The working fluid mainly used is deionized water and copper material is widely used for the vapor chamber and heat pipe. There is no hard line in the difference between a vapor chamber or heat pipe. However, we can distinguish the two in terms of heat moving or heat spreading. The heat pipe mainly transfers heat from the source to the remote condenser thus providing linear flow or one dimensional heat flow. On the other hand, vapor chamber spreads heat in all directions as it is mounted directly on the heat source. Thus it provides multidirectional heat flow. The length of the heat pipe is much greater than the pipe thickness whereas the surface area of vapor chamber is much bigger than vapor chamber thickness. The vapor chamber integrated with heat sink is directly mounted on the heat source i.e. chip. Therefore, the lower copper wall in

contact with the chip is hotter surface is called as evaporator side and the upper copper wall which carries the heat sink (cooler region) is called as condenser side. There is a thermal interface material between the evaporator side of vapor chamber and the chip surface. This facilitates the elimination of air gaps and minimizes contact resistance.

2.2 Types of Wick Structures

The performance of a heat pipe/ vapor chamber depends on several factors, one of which is the nature of the wick structure. To optimize the thermal performance of these devices requires wick structures that can provide high capillary pressure, high permeability and yet still offer low resistance to fluid flow. It should also provide greater meniscus area to sustain thin-film evaporation. Also the factors such as the different power density handling capacity, orientation in which they are employed and the thermal resistance offered by the wick structures should be considered while selecting a wick structure. The three different types of wick structures widely used are sintered wick, grooved wick and screen wick. The figure 2-3 shows schematic representation of these wick structures.

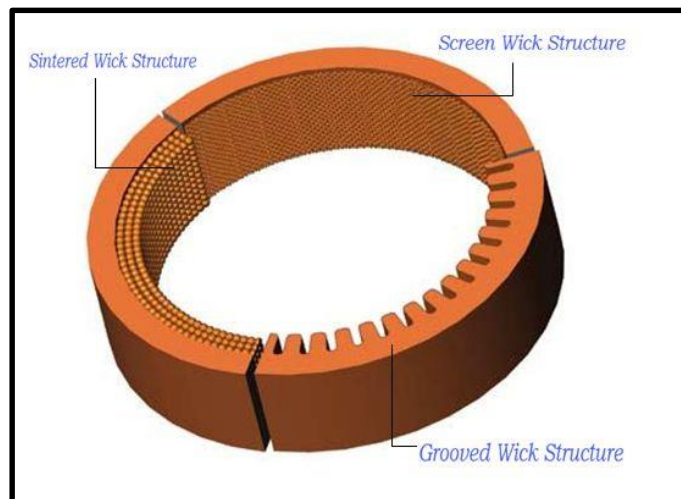


Figure: 2-3 Types of wick structure

2.2.1 *Sintered Wick*

The sintered wick is most widely used wick structure in the market place. In this design powdered metal is bonded and hardened to the internal pipe walls [2]. Copper powder is the most widely used material for this wick structure. It is most resistant to the heat source orientation and gravity. It also offers strongest capillary action among the three designs and is the most expensive wick structure.

2.2.2 *Mesh or Grooved Wick*

This wick is used when the heat source is in level with the condenser or above the condenser. Extrusion or threading processes are used to produce grooves in aluminum or copper tubing. The chief benefit of using such design is reduced cost and ease of producing extremely thin wick designs.

2.2.3 *Screen Wick*

In this design a metal is wrapped tightly along a mandrel and inserted inside an aluminum or copper tube i.e. heat pipe. Then the mandrel is removed from the tube keeping the wrapped metal aligned with the tube due to tension in the wrapped metal. The porosity of the metal wrap determines the performance of the wick structure.

The basic function of wick structure remains the same i.e. to develop capillary action for the liquid returning from the condenser (heat output/heat sink) to the evaporator (heat input/source). The sintered wick design works well with bent shapes without affecting its performance. Thus when heat needs to be moved from one point to another point heat pipes usually use sintered wick structure due to no limitations in bending. Following table shows the different characteristics for the three wick structures.

Table 2-1 Properties of different wick structures

Wick Type	Power Density	Resistance	Orientation
Sintered Wick	< 500 w/cm ²	0.15-0.03 °c/w/cm ²	+90° to - 90°
Mesh or Grooved Wick	<30 w/cm ²	0.25-0.15 °c/w/cm ²	+90° to - 5°
Screen Wick	<20 w/cm ²	0.35-0.22 °c/w/cm ²	+90° to -0°

2.3 Effective Thermal Conductivity of Wick Structure

The wick saturated with water should vaporize when heat is applied so that the evaporation process is completed successfully. The low thermal conductivity of water compared to higher thermal conductivity of copper powder becomes a thermal barrier. There are many methods to calculate the effective thermal conductivity of wick structure. For parallel assumption, effective thermal conductivity wick can be calculated as given below:

$$K_w = (1 - \epsilon)K_s + \epsilon K_l \quad (1)$$

For series assumption, effective thermal conductivity wick can be calculated as given below:

$$K_w = \frac{1}{\frac{(1 - \epsilon)}{K_s} + \frac{\epsilon}{K_l}} \quad (2)$$

For effective thermal conductivity sintered wick structure, the relation is given by Maxwell [3] as,

$$K_w = K_s \left[\frac{2 + \frac{K_l}{K_s} - 2\epsilon \left(1 - \frac{K_l}{K_s}\right)}{2 + \frac{K_l}{K_s} + \epsilon \left(1 - \frac{K_l}{K_s}\right)} \right] \quad (3)$$

In the above equations, K_l is thermal conductivity of water

K_s is thermal conductivity of copper

ϵ is the porosity of wick

The table 2-2 gives the values of wick thermal conductivity calculated by using the above three equations.

Table 2-2 Values of effective wick thermal conductivity

Equation (1)	Equation (2)	Equation (3)
192.8	1.19	152.8

It is safe to assume the value of effective wick thermal conductivity within the range of these equations for our computational fluid dynamics analysis. The value used in Grubb [4] and Vadakkan et al. [5] is taken as 40 W/mK. However, a more conservative approach is applied in selecting conductivity value of wick and is set to be 30 W/mK. Our baseline CFD model of vapor chamber with micro pillar has 34 nos. of micro pillars with 50 microns width each, and is made up of sintered wick material [6]. This wick structure is in addition with the bottom layer sintered wick placed on lower copper wall of vapor chamber.

2.4 Types of Working Fluid

A vapor chamber is a two phase device which transfers heat by using a working fluid. This working fluid serves as a medium to transfer heat by changing its phase from liquid to vapor and again from vapor to liquid. The choice of working fluid to be used depends on many factors such as, the operating temperature range of the equipment, vapor pressure of the working fluid and the required latent heat of vaporization as per the application. We know that the boiling of a liquid is a temperature at which vapor pressure of the liquid equals the surrounding pressure of the liquid. The vapor pressure is an indication of a liquid's evaporation rate. The boiling point of liquid is low as lower pressures. The broadly accepted operating temperature range commercial electronic devices is in between 0°C -70°C. Therefore, for evaporation take place our working fluid should have a boiling point falling in this range. The high thermal performance of vapor chamber is due to high latent heat of vaporization of the working fluid.

The table 2-3 shows most commonly used working fluids and their desirable properties. It can be seen that every application demands a different working fluid.

Table 2-3 Types of working fluids used in two phase devices

Working Fluid	Boiling Point(°C) at Atmospheric Pressure (101 kPa)	Vapor Pressure (kPa) at T_{sat} 45°C	Latent Heat of Vaporization (KJ/KG)
<u>Water</u>	<u>100</u>	<u>9.59</u>	<u>2264.76</u>
Methanol	64.7	44.47	1104
Acetone	56	67.91	518
Ammonia	-33.34	1578.9	1369

From the table is clear that working fluid should have a boiling point within the operating temperature range of the electronic device. We know that at lower pressures the boiling point of liquid is lowered. Due to the presence of vacuum in the vapor chamber the boiling point of liquid is much lower than that at atmospheric pressure. We have selected water as the best choice of working fluid for our application. This is because at temperature of 45°C in the heat spreader section of our model water has a vapor pressure of 9.59 kPa which falls in lower vacuum range. Also it offers high latent heat of vaporization of 2264.76 KJ/KG which offers high thermal performance.

In addition to above properties following factors also contribute significantly towards the choice of working fluid. They are listed as compatibility with wick and wall materials, good thermal stability, and wettability of wick and wall materials, high surface tension, high latent heat, low liquid and vapor viscosities, and high thermal conductivity.

2.5 Effective Thermal Conductivity of Vapor Space

According to Prasher [7], in the case of remote cooling mode the effective vapor thermal conductivity of vapor space can be calculated by using following formula given below:

$$K_{vapor} = \frac{L^2 p_v \rho_v d_v^2}{12 R \mu_v T^2}$$

In the above equation we have,

L = latent heat of vaporization (J/kg)

p_v = vapor pressure (N/m²)

ρ_v = density of vapor (kg/m³)

d_v = thickness of vapor space (m)

R = gas constant per unit mass (J/kg)

μ_v = viscosity of vapor (kg/ms)

T = temperature (K)

The above equation is derived by using ideal gas law equation and Clausius Clapeyron equation for incompressible laminar flow. However, vapor thermal conductivity is not easy to be defined in the case of active cooling mode. In our study the vapor chamber is set in active cooling mode and vapor is being used as a heat spreader. Therefore, after a certain value the heat spreading will be independent of the effective thermal conductivity of vapor. Thus it is safe to assume a high value of vapor thermal conductivity for thermal simulations. The experimental results show that the vapor thermal conductivity can be as high as 30000 W/mK [6]. Also it has been observed that changes in the value of vapor thermal conductivity has no significant effect in overall thermal performance of the model.

In our current CFD model of vapor chamber with micro pillars we have 35 nos. of vapor spaces which are part of heat spreader along with wick micro pillars. These vapor spaces act as heat spreader with vapor thermal conductivity of 30000 W/mK for each vapor space.

Chapter 3

Computational Fluid Dynamics (CFD) Study

3.1 Introduction

The computational fluid dynamics is often abbreviated as CFD is a branch of fluid mechanics that uses numerical analysis and algorithms to solve and analyze problems that involve fluid flows. It uses applied mathematics, physics and computational software to predict the behavior of a fluid in particular medium, also the behavior of fluid flowing over an object.

Mainly computational fluid dynamics is based on Navier-Stokes equation which describes the velocity, pressure, temperature, and density of flowing fluid. We can run the simulations and analyze parameters these according to user's point of interest within the domain and see the result of the projects [8]. In current work, ANSYS Icepak was used to model the vapor chamber with micro pillars as well as to model copper spreader design. The primary focus was given to chip junction temperature in both of the cases. ANSYS Icepak is generally used to simulate electronic cooling strategies and overall electronic thermal management for IC packages, PCB and electronic assemblies.

3.2 Methodology

There are many CFD software's commercially available in market to solve our simulation needs and perform fluid flow analysis. However, they follow a similar method in defining the problem and solving it. The general procedure followed by the CFD software ANSYS-Icepak [9] is briefly mentioned below:

Step 1: Geometry

The geometry can be imported in the form IGES, STEP, IDF formats or we can use object based model building with predefined objects such as cabinets, blocks, heat exchangers, enclosures, grilles, sources etc.

Step 2: Mesh

Automatic unstructured mesh is generated having hexahedra, tetrahedra, pyramids, prisms, and mixed element mesh types pyramid. User can further check the mesh quality and go for coarse mesh generation or non-conformal meshing.

Step 3: Materials

The model created or imported has to be assigned with respective material properties to each part of the model. ANSYS-Icepak provides a comprehensive material property database, along with temperature dependent material properties to select the materials. User can also create a new material and define properties as per his choice.

Step 4: Physical Models

The user sets up the laminar or turbulent flow model for the design. Also specifies the type of analysis needs to be performed such as steady state analysis or transient. The user also has to specify the type of heat transfer mode involved i.e. conduction, forced, natural or mixed-convection, radiation.

Step 5: Boundary Conditions

Openings and grilles with specifications of inlet/exit velocity, exit static pressure, inlet pressure, inlet temperature etc. is defined by the user.

Step 6: Solver

ANSYS-Icepak uses Fluent, a finite volume solver as his solver engine to perform the simulation. The solver includes pressure based solution algorithm with sophisticated multigrid solver scheme to reduce computational time.

Step 7: Visualization

User can visualize velocity vectors, contours, particle traces, grid, cut planes and isosurfaces. The contours of velocity components, speed, temperature, species mass fractions, pressure, heat flux, heat transfer coefficient, flow rate, turbulence parameters provide much better and detailed understanding of the model behavior.

Step 8: Reporting

The performed simulations are written to user-specified ASCII files for all solved quantities and derived quantities. These quantities can be on all objects, parts of objects and the user-specified regions of domain.

Chapter 4

Computational Fluid Dynamics (CFD) Modeling of Vapor Chamber with Micro Pillars

4.1 Model Setup in ANSYS-Icepak

A 3-D model of vapor chamber with micro-pillar is modelled by using ANSYS-Icepak. The model is baselined so as to compare its thermal performance with copper spreader model which is designed in ANSYS-Icepak as well. Further a parametric study is carried out for the baseline model to explore the performance limits vapor chamber. The designed baseline model is shown in figure 4-1 given below.

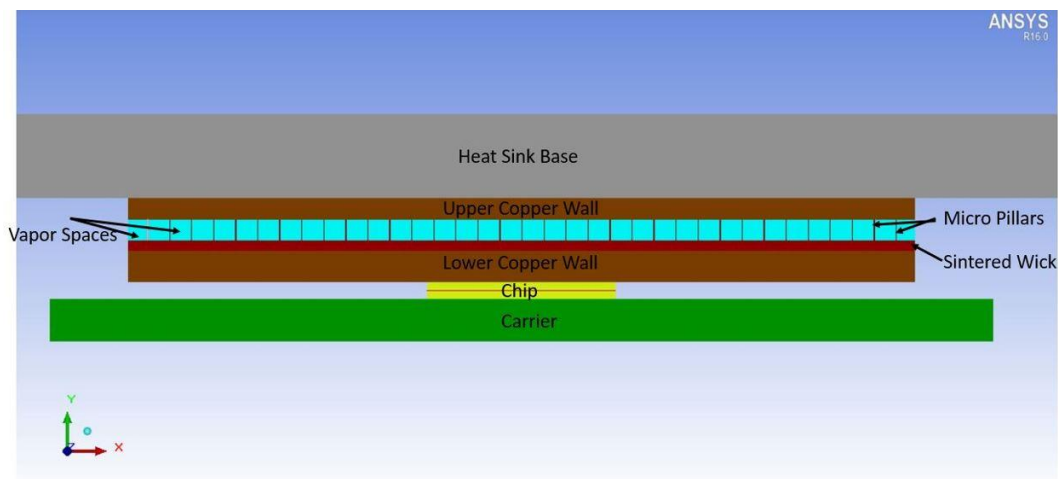


Figure 4-1 CFD Model of Vapor Chamber with Micro Pillar

In the above model we have solder plus under fill in between the chip bottom surface and carrier top surface. Further there is thermal interface material or thermal grease in between the chip top surface and bottom of lower copper wall. There is another thermal interface material between the top surface of upper copper wall and heat sink bottom surface. Also the heat spreader consists of 34 wick micro pillars and 35 vapor spaces for baseline model. A layer of sintered wick is present on top of the lower copper wall which performs the capillary action along with the wick micro pillar structures.

The model consists of several components, these components are of different dimensions and possess different material properties. The table 4 shows the dimensions of various parts of the model, their corresponding material properties and shapes.

Table 4-1 Material properties and dimensions of different parts of the vapor chamber with micro pillars model (baseline study)

Part	Shape	Material/Thermal Conductivity (W/m-K)	Dimensions (mm)
Carrier	Block	Ceramic/21	45X45X2
TIM 1	Plate	Solder + Under fill/5	9X9
Chip	Block	Silicon/180	9X9X0.785
TIM 2	Plate	Thermal Paste/3.8	9X9
Lower Copper Wall	Block	Copper/387.6	37.5X37.5X1.5
Sintered Wick	Block	Sintered Copper Powder/30	37.5X37.5X0.5
Micro Pillars (34 nos.)	Block	Sintered Copper Powder/30	0.05X37.5X1
Vapor Spaces (35 nos.)	Block	Water Vapor/30000	1X37.5X1
Upper Copper Wall	Block	Copper/387.6	37.5X37.5X1
TIM 3	Plate	Thermal paste/3.8	37.5X37.5
Heat Sink Base	Block	Aluminum/240	90X90X4

The heat source has Thermal Design Power (TDP) of 100 W is placed at the center of the chip. The wick thermal conductivity is calculated using the formulas mentioned in section 2.3 Effective Thermal Conductivity of Wick Structure. The wick thermal conductivity is set as 30 W/m-K and vapor thermal conductivity is taken as 30000 W/m-K.

4.2 Part Modeling in ANSYS-Icepak

The object creation toolbar in ASYS-Icepak provides various options to design a model of our own choice. It also provides an alternative to modify the existing objects as per the requirement of user. Each object comes with its own attributes in terms of geometry, thermal behavior, boundary conditions and material properties etc. Thus we need to take in consideration that the object we select suffices our application with an accountability of the required properties set by the user.

A brief description is given below about the objects used to create vapor chamber with micro pillar model (baseline case) and simple copper spreader model [9].

4.2.1 *Cabinet:*

The cabinet is the first and foremost object created by ANSYS-Icepak. The default geometry of cabinet is 1mX1mX1m 3D rectangular cabinet. The sides of the cabinet represent the physical boundary of the model and no object can extend outside the cabinet. The wall types that can be assigned is wall, opening, and grille. The cabinet can be resized according the user's preference. In this case the cabinet was set to open on all sides as we are dealing with only conduction mode of heat transfer. This is done by setting the shape of cabinet as none instead of open.

4.2.2 *Block:*

The default shape of block is taken as prism whereas we can change the shape as per our choice. Also the default block type is set as solid which can be changed into hollow, fluid, or network. The model uses solid prism block for objects such as carrier, chip, lower copper wall, sintered wick, micro pillars, vapor spaces, upper copper wall and heat sink base. They possess physical and thermal characteristics such as density,

specific heat, thermal conductivity and total heat flux. The vapor spaces and the wick micro pillars constitute the heat spreader area and are the regions of high heat conduction in the design. The heat sink base top was given a convective heat transfer coefficient of $1400 \text{ W/m}^2\text{K}$.

4.2.3 *Plate:*

Plates are objects that are impervious to fluid flow. The plate geometries include adiabatic thin, conducting thick, conducting thin, hollow thick or contact resistance. The plates in the model were used to design TIM 1, TIM 2, and TIM 3 parts of the model. They were modeled as conducting thin plates. They can conduct heat in either direction and have no physical thickness. They can possess only effective thickness. The main purpose of using thermal interface is to minimize the contact resistance and avoid air gaps between the interface of different materials. Also they conduct heat in very small amounts along their surface.

4.2.4 *Source:*

The source represents areas in the model which can generate energy. The energy sources can be given thermal condition as total power, surface/volume heat flux, or fixed temperature. The only part in the model which can generate heat is chip. The chip is made up of silicon material which generates heat at total power of 100 W for the given model. The heat source is placed at the geometric center of the chip and is rectangular in shape. The simulation is done for steady state analysis therefore we have a constant heat source.

4.3 Analysis Setup

After creating the geometry and finishing design model a computational mesh has to be generated which forms the basis of solution procedure. The following section talks about the steps to be taken to setup the problem.

4.3.1 *Generating Mesh*

A good computational mesh is essential for accurate solution. If the mesh is coarse the accuracy of solution is adversely affected whereas if the mesh is too fine the computational cost is high. Therefore, there has to be a trade-off in between these extremes to have an optimum mesh quality. The following mesh parameters were set for the simulation;

- Mesh type: Mesher HD
- Max element size: 1.5mm
- Mesh parameters: Normal
- Minimum elements in gap: 3
- Minimum elements on edge: 2
- Max size ratio: 2
- Number of elements: 358194

4.3.2 *Basic Parameters*

- Variables solved: Temperature
- Radiation: Off
- Flow regime: Turbulent (zero equation)
- Time variation: Steady (steady state analysis)
- Ambient Temperature: 35° C

4.3.3 Solution Settings

Energy convergence criteria: $1e-14$

Discretization Scheme for temperature: First

Temperature Solver Type: W

Precision: Double

4.4 Analysis Results

4.4.1 Contour Plots: Plane Cut Temperatures

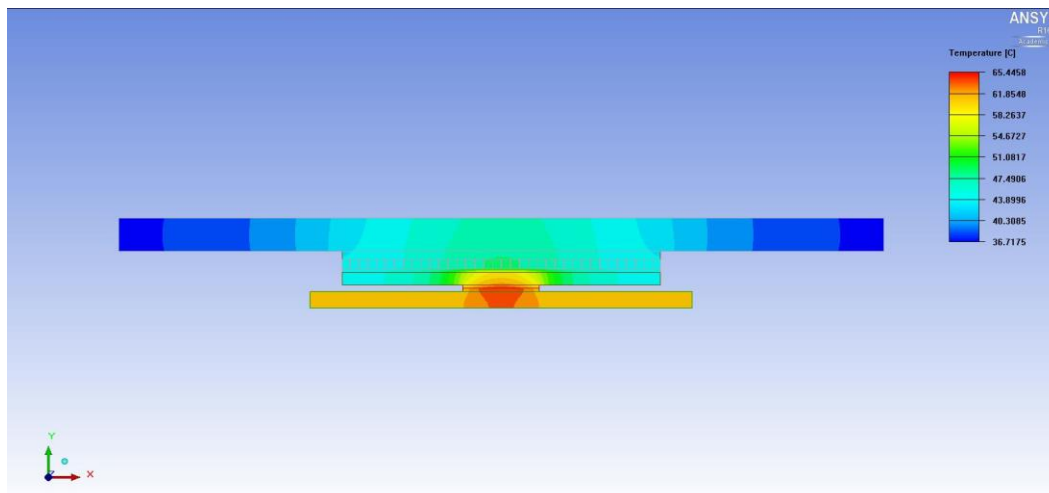


Fig 4-2 Plane cut temperature for vapor chamber with micro pillars model

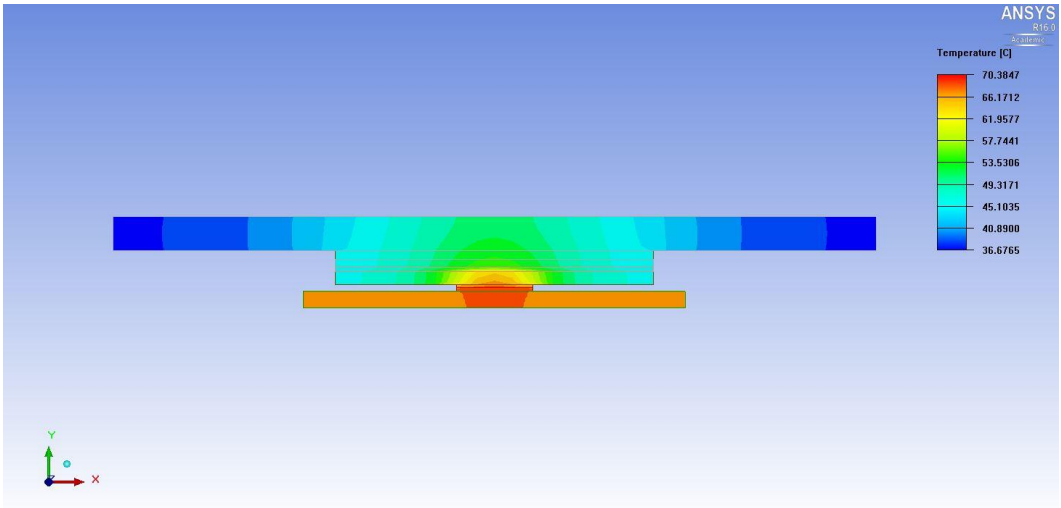
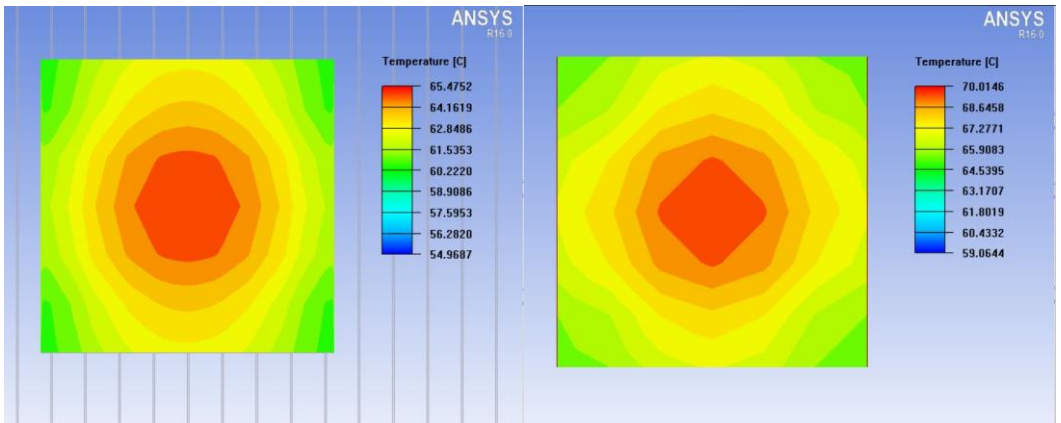


Fig 4-3 Plane cut temperature for copper spreader model

4.4.2 Temperature Contours



(a) Vapor Chamber with Micro Pillars

(b) Copper Spreader

Fig 4-4 Top surface temperature distribution of chip surface

The fig 4-4 shows the temperature contours of top surface of the chip as observed in both the cases. It can be seen that the junction temperature of the chip in

case of vapor chamber with micro pillars model is 5°C lower than that of copper spreader model. Also the junction-to-ambient thermal resistance is calculated to be $\theta_{JA} = 0.304$ °C/W for vapor chamber with micro pillars whereas for copper spreader model $\theta_{JA} = 0.354$ °C/W. Therefore, it can be concluded that the thermal resistance of vapor chamber model is found to be 14% lesser than that copper spreader model.

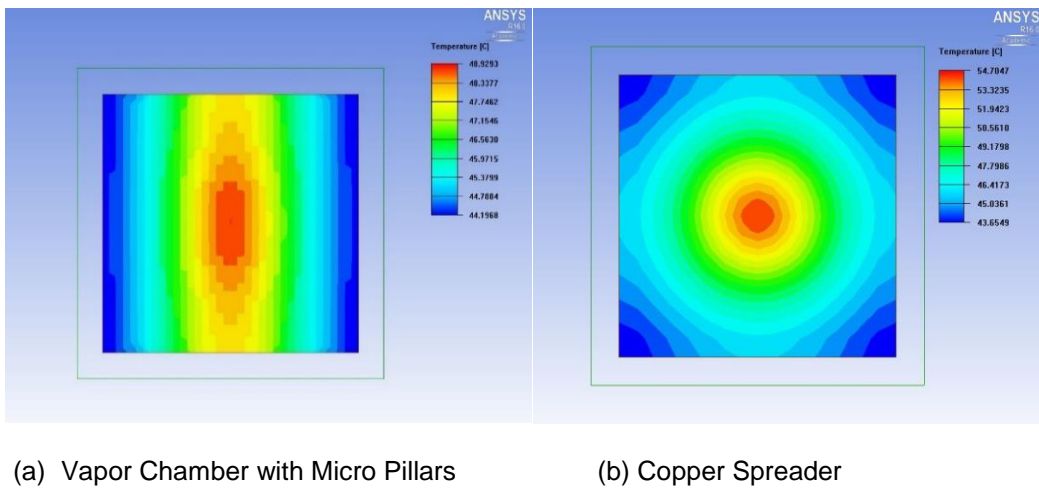


Fig 4-5 Top surface temperature distribution of heat spreader

The fig 4-5 shows the temperature distribution of the heat spreader section of both the models. In case of vapor chamber with micro pillars model the heat spreader consists of vapor spaces and wick micro pillars. For the copper spreader model the rectangular copper block is the heat spreader. It can be seen from the fig 4-5 shows that the top surface of vapor chamber model is ~6°C lower than copper spreader model. Also there is large temperature variation in case of copper spreader model of 11°C whereas for the vapor chamber with micro pillars model it is approximately ~5°C.

4.5 Intel 6th Generation Core i7 Chipset

The chip designed in baseline model and spreader model is in reference with the intel's core i7 chipset. The dimensions for the chip were selected similar to that of intel 6th generation core i7 chip. The thermal profile of intel 6th generation i7 thermal test vehicle (TTV) data was compared with the thermal profile behavior of vapor chamber model with micro pillars and copper spreader model. The comparison was done between these three thermal profiles at same ambient temperature and thermal design powers and corresponding case temperatures was observed.

4.5.1 Thermal Profile

All thermal profiles follow the linear equation format, $y = mx + b$.

Where,

y = temperature (T) in °C

m = slope ψ_{CA} (CA=case to ambient)

x = power (P) in Watts (W)

b = y-intercept (T_{LA}) °C (LA=local ambient)

The fig 4-6 shows the thermal profile of intel's core i7 PCG 2015D processor [10] and fig 4-7 shows the thermal profiles of the CFD models. The objective is to validate the case temperatures observed in vapor chamber with micro pillars model concurs with that of intel's TTV thermal profile. For validation analysis the ambient temperature was set to 43.7°C and case temperatures were observed by varying the thermal design power.

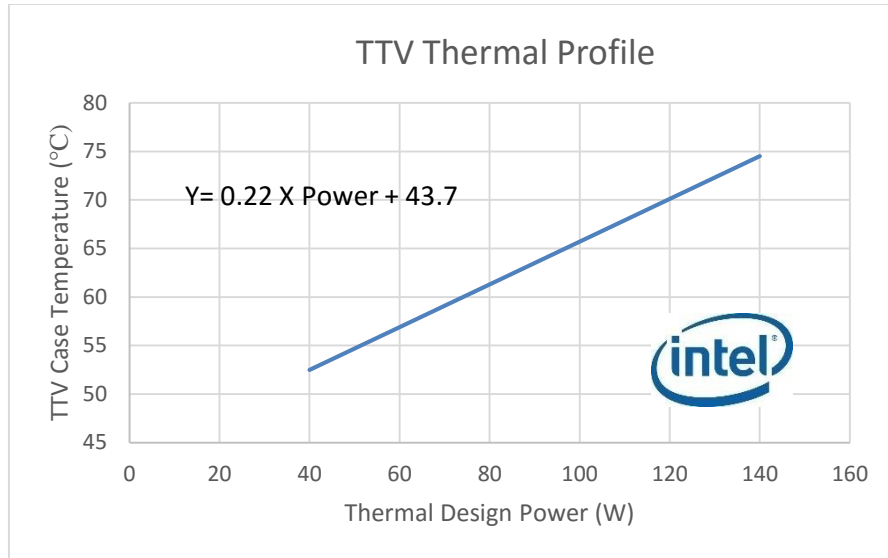


Fig 4-6 Thermal profile of intel 6th gen core i7 TTV

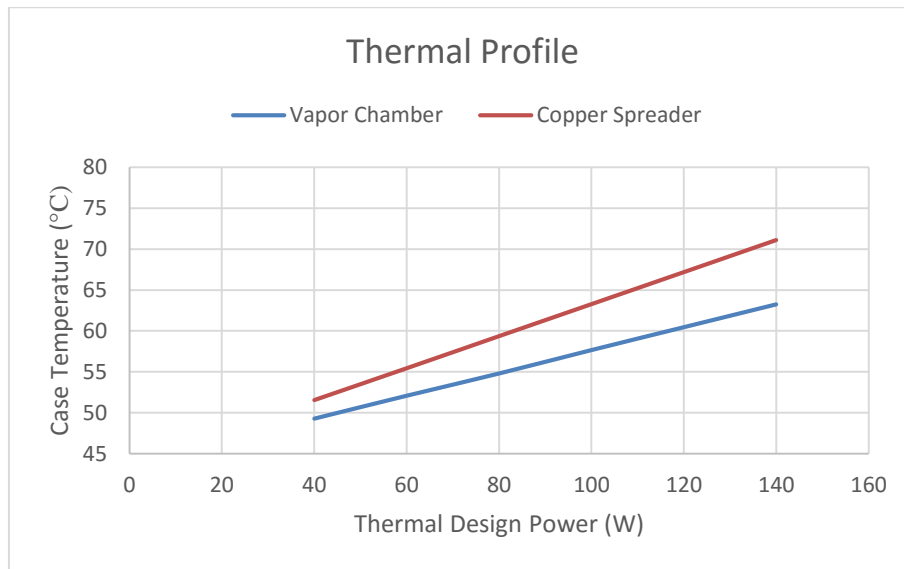


Fig 4-7 Thermal profile vapor chamber model and copper spreader model

From the fig 4-6 and fig 4-7 it can be seen that at any given thermal design power the case temperature in the case of vapor chamber model with micro pillars

is lowest. Also the thermal profile of copper spreader model closely matches to the intel's TTV thermal profile. Thus the vapor chamber with micro pillar model offers high performance thermal behavior and concurs with intel's TTV case temperatures at a given thermal design power.

Chapter 5

Parametric Study of Vapor Chamber with Micro Pillars

A parametric study was conducted to analyze the thermal performance of vapor chamber with micro pillars. The objective of the study is to examine the factors affecting the thermal performance of the vapor chamber and to explore the design space available to design the vapor chamber. This is done by varying certain parameters of the original model. The factors that are varied include,

- Power/heat flux (section 4.5)
- Heat spreader width
- Effective thermal conductivity of wick and vapor space
- Convective heat transfer coefficient of heat sink base
- Heat sink size

5.1 Effect of changes in heat spreader width

The heat spreader width is varied for both the models the vapor chamber with micro pillars and copper spreader model. The heat spreader is a square block of 37.5mm x 37.5mm in baseline study. It is varied by changing the dimensions of the square in steps of 5mm x 5mm. The corresponding junction and case temperatures is observed for both models for varying heat spreader width. The fig 5-1 shows the effect of changes in heat spreader width on the junction and case temperatures. It can be seen that as the spreader width increases both junction as well as the case temperatures decreases for both the models. Also at smaller spreader width the copper spreader model outperforms the vapor chamber with micro pillar model. However, as the spreader width increases the vapor chamber outperforms the copper spreader model. The cross over point approximately occurs at about 13mm x 13mm.

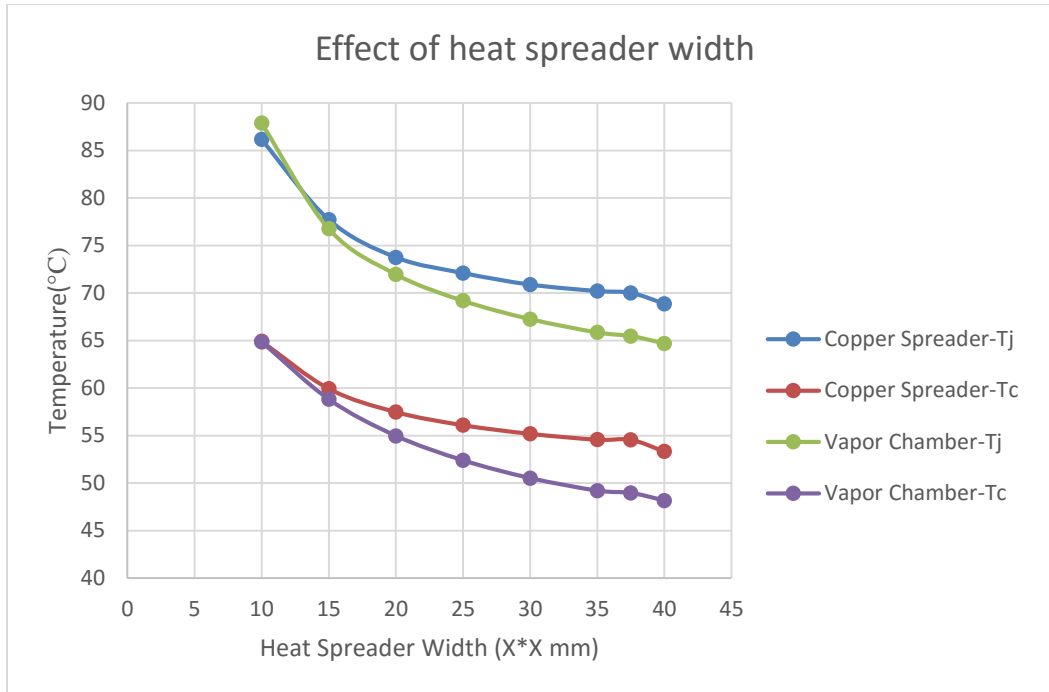


Fig 5-1 Effect of heat spreader width on junction and case temperature on vapor chamber with micro pillars model and copper spreader model

From the fig 5-1 it can be concluded that vapor chamber with micro pillars serves effective heat spreading over large area compared to that of solid copper metal block. Thus, it can be used in applications where large area is involved with low heat transfer coefficient.

5.2 Effect of effective thermal conductivity of wick and vapor space

The values of thermal conductivity of wick and vapor space are based on experimental data and the formulae's used to calculate them are based on assumptions which are not accurate. Thus we have a range in which these values usually lie.

Therefore, its necessary to select appropriate effective thermal conductivity for the wick and vapor space.

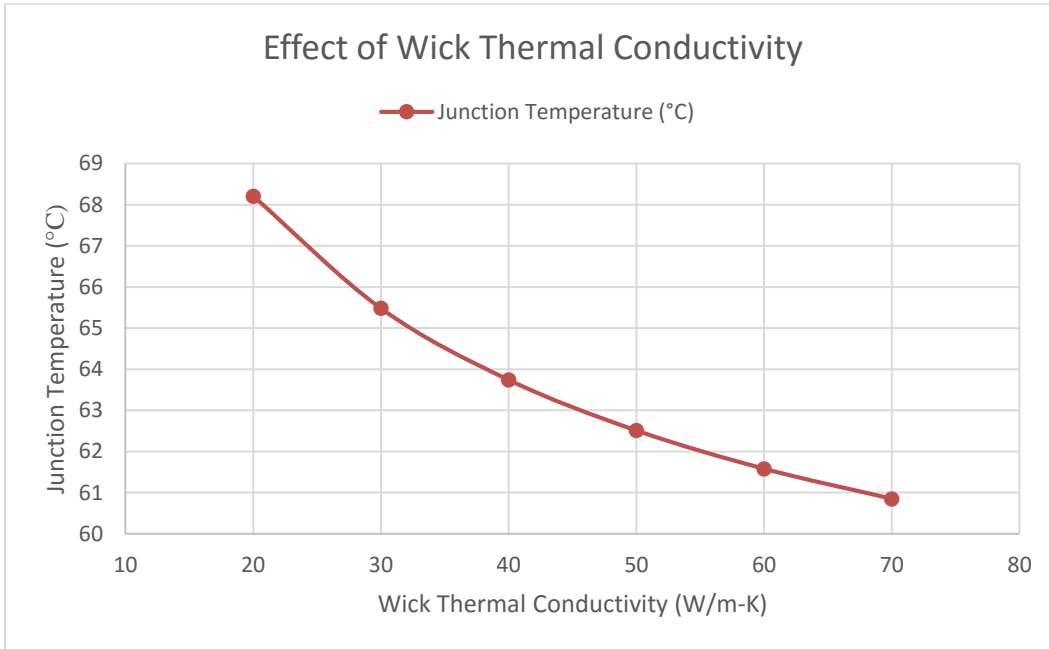


Fig 5-2 Effect of wick thermal conductivity on junction temperature of vapor chamber with micro pillars model

The fig 5-2 shows the variation in the junction temperature of vapor chamber with micro pillars model with a change in the wick thermal conductivity value whereas the vapor thermal conductivity value was fixed to be 30000 W/m-K. The junction temperature decreases drastically with the increase in wick thermal conductivity. Thus a more conservative approach should be adopted while selecting wick thermal conductivity value. The value of wick thermal conductivity was changed in the steps of 10 W/m-K and corresponding junction temperatures were noted.

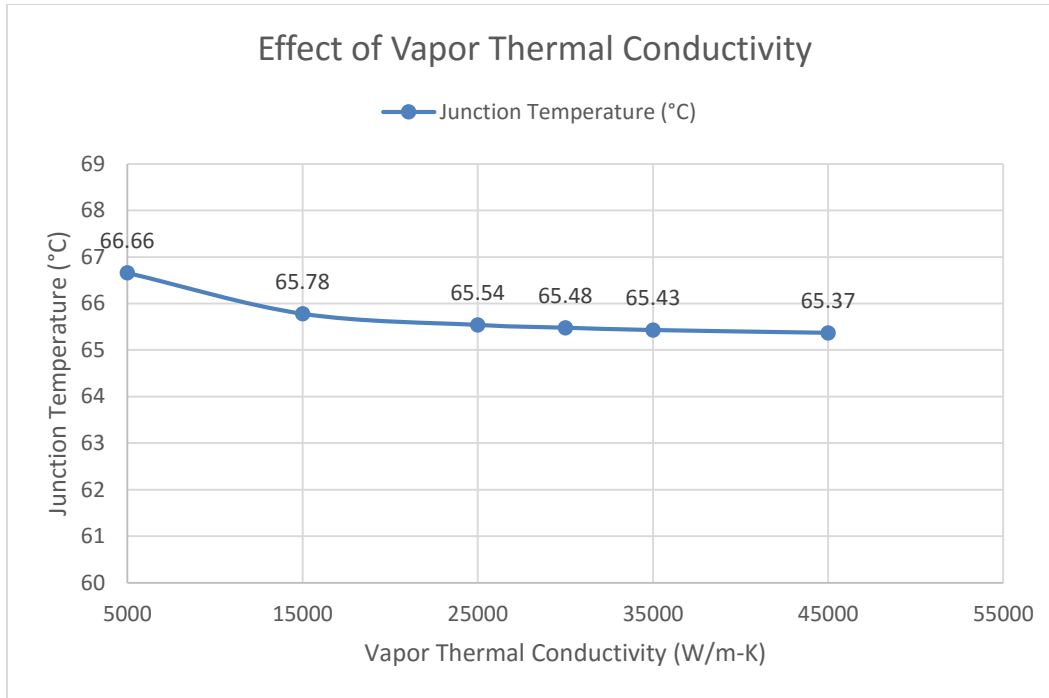


Fig 5-3 Effect of vapor thermal conductivity on junction temperature of vapor chamber with micro pillars model

The fig 5-3 shows the variation in the junction temperature of vapor chamber with micro pillars model with a change in the vapor thermal conductivity value whereas the wick thermal conductivity value was fixed to be 30 W/m-K. It was observed that junction temperature did not decrease noticeably with the increase in vapor thermal conductivity as did it for wick thermal conductivity. The value of wick vapor thermal conductivity was changed in the steps of 10000 W/m-K and corresponding junction temperatures were noted.

Thus from fig 5-2 and fig 5-3 we can conclude that effective wick thermal conductivity has more pronounced effects on the thermal performance of the vapor chamber with micro pillars model than that of effective vapor thermal conductivity.

5.3 Effect of convective heat transfer coefficient of heat sink base

In the baseline study an effective heat transfer coefficient of 1400 W/m²K is applied to the top surface of the heat sink base. The heat sink on the vapor chamber model is basically the condenser region of the vapor chamber. The fig 5-4 and fig 5-5 shows the effect of convective heat transfer coefficient of heat sink base on the junction and case temperatures of vapor chamber model and copper spreader model.

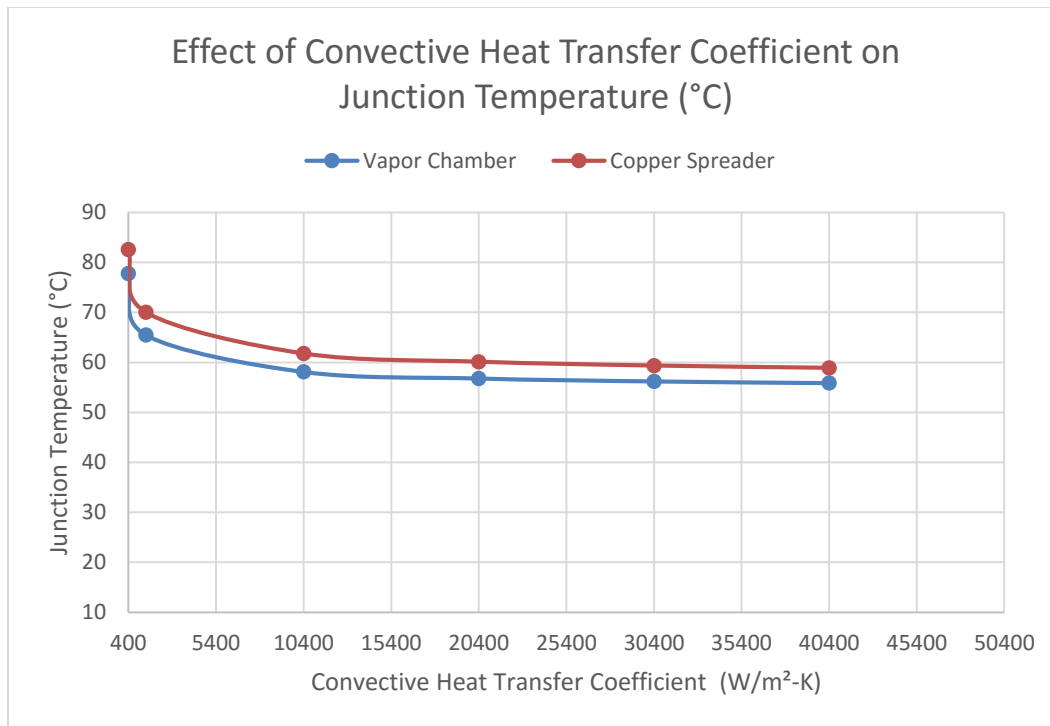


Fig 5-4 Effect of convective heat transfer coefficient on junction temperature

The fig 5-4 shows the effect of convective heat transfer coefficient on junction temperature of vapor chamber with micro pillars model and copper spreader model. It is observed that the junction temperature decreases for both the models as the convective heat transfer coefficient increases.

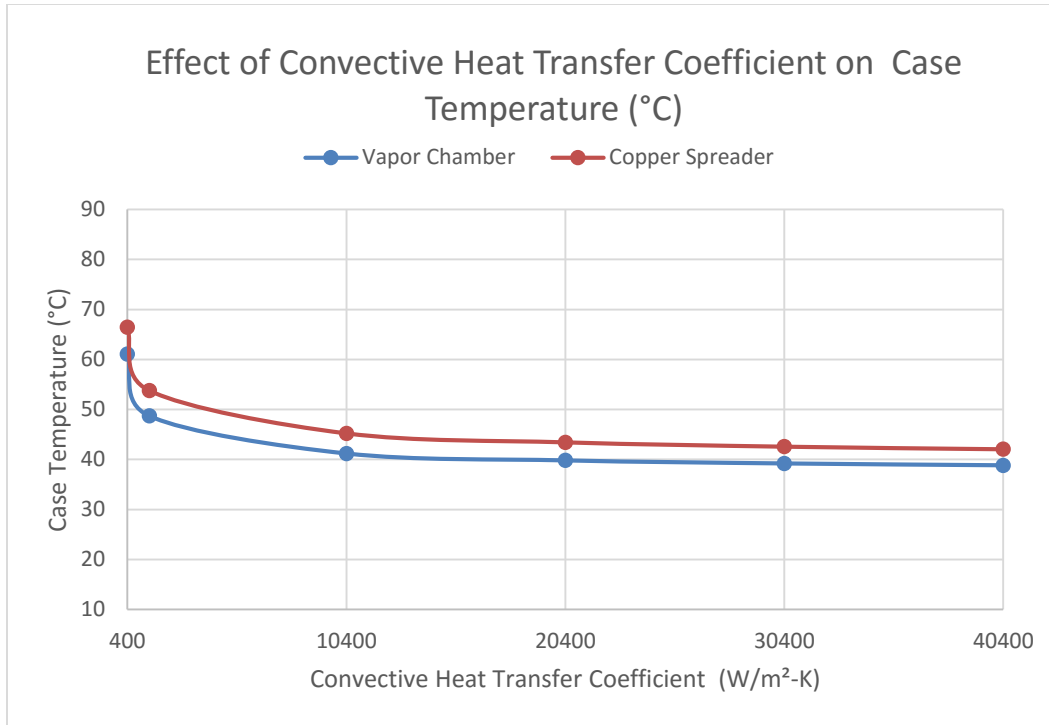


Fig 5-5 Effect of convective heat transfer coefficient on case temperature

The fig 5-4 shows the effect of convective heat transfer coefficient on junction temperature of vapor chamber with micro pillars model and copper spreader model. It is observed that the junction temperature decreases for both the models as the convective heat transfer coefficient increases.

5.4 Effect of heat sink base size

The heat sinks transfer the thermal energy from high temperature device to lower temperature fluid medium such as air or liquid. The heat transfer capability is affected by the surface area in contact with the surrounding fluid. The greater heat sink size comes with increased weight and cost to the design. Thus heat sink size should provide high thermal performance simultaneously with light weight and lower cost.

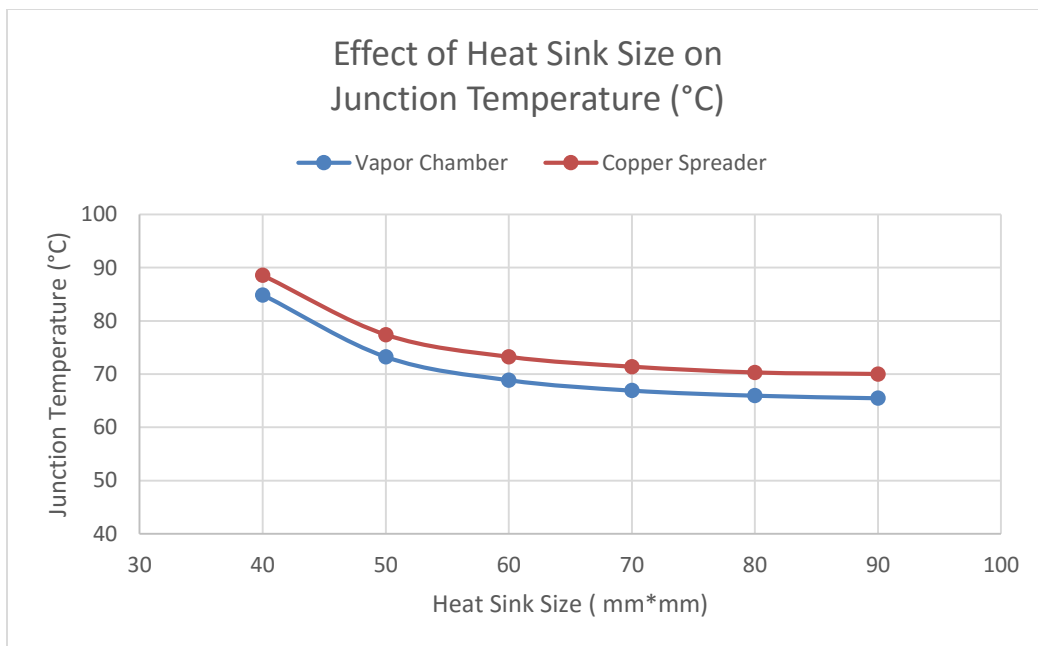


Fig 5-6 Effect of heat sink base size on junction temperature

The fig 5-6 shows the effect of heat sink base size on the junction temperature of vapor chamber with micro pillars model and copper spreader model. It is observed that the junction temperature for both the models decrease with increase in heat base sink size. This is expected since greater the surface area available to transfer heat lower the junction temperature of the model.

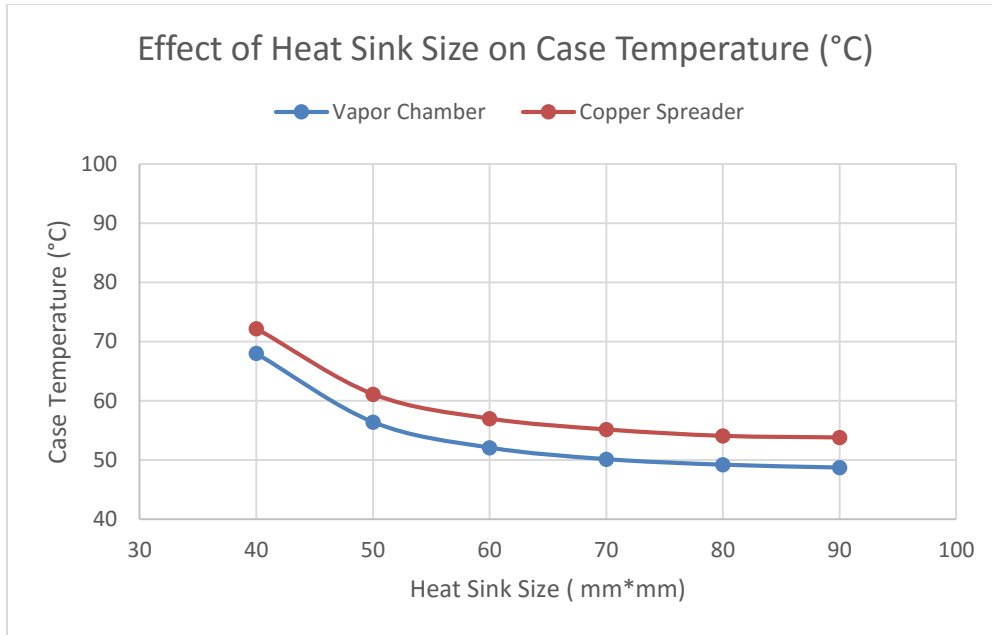


Fig 5-7 Effect of heat sink base size on case temperature

The fig 5-7 shows the effect of heat sink base size on the case temperature of vapor chamber with micro pillars model and copper spreader model. It is observed that the case temperature for both the models decrease with increase in heat base sink size.

Therefore, we can use heat sink of smaller size and weight and achieve required junction and case temperatures by inserting vapor chamber below the heat sink instead of using solid metal block as heat spreader.

Chapter 6

Conclusion

6.1 Summary

The two phase devices exhibit superior thermal performance over solid metal heat spreaders for the current application. The CFD analysis of vapor chamber with micro pillars showed lesser thermal resistance ($\theta_{JA} = 0.304^{\circ}\text{C/W}$) than that of copper heat spreader model ($\theta_{JA} = 0.354^{\circ}\text{C/W}$). On comparison it was observed that the vapor chamber with micro pillars model offered 14% lesser thermal resistance than that offered by the copper spreader model. The plane cut temperature contours of vapor chamber with micro pillars model showed reduction in the hot spots. The CFD model of vapor chamber with micro pillars concurs with Intel's TTV data of i7 chipset.

The factors affecting the thermal performance of vapor chamber with micro pillars were studied by performing CFD analysis. Furthermore, a parametric study was performed to observe the thermal behavior of the vapor chamber model and was compared with that of copper spreader model. Based on the results following conclusions were drawn.

- The junction temperature rise with increase in power input, is higher in copper spreader model than the vapor chamber.
- For smaller heat spreader width copper model outperforms the vapor chamber with micro pillars model, but for larger spreader widths vapor chamber performs way better than copper model. The cross over point occurs approximately at 13mm x 13mm.
- The wick thermal conductivity significantly affects the thermal performance than the vapor thermal conductivity.

- The hot spots over the semiconductor die spread out due to insertion of vapor chamber at the base of heat sink.
- Increasing convective heat transfer coefficient of heat sink base results equally beneficial for the vapor chamber with micro pillars model as well as for the copper spreader model.

6.2 Future Work

The obtained computational fluid dynamics (CFD) simulation results can be compared with the experimental setup and the degree of accuracy of the results can be calculated. This will help in determining the deviations if found, and the science behind it. Also the wick structures used, need enhancement in terms of the capillary limit and precise value of the effective thermal conductivity. An incisive two phase CFD simulation can give more lucid picture of the thermal behavior of the model and the phase change transformation of the working fluid into vapor and back and forth.

References

- [1] J. H. Lau. 1995. Ball Grid Array Technology. New York: McGraw-Hill.
- [2] S. V Garimella, J. A. Weibel, "Recent advances in vapor chamber transport characterization for high heat flux applications", CTRC research publications, 2013.
- [3] Maxwell J.C., A Treatise on Electricity and Magnetism, Vol. 1, 3rd edition, reprinted by Dover, New York, 1954.
- [4] Grubb K., "CFD Modeling of a Thermo-Base Heat Sink", 8th International FLOTHERM User Conference, Las Vegas, USA, 13-14, May 1999.
- [5] Vadakkan U., Chrysler G., and Sane S., 2005, "Silicon/Water Vapor Chamber as Heat Spreaders for Microelectronic Packages", IEEE SEMI-THERM Symposium, pp. 182-186, Mar 2005.
- [6] Yasuhiro Horiuchi, Masataka Mochizuki, Koichi Mashiko, Yuji Saito, Fumitoshi Kiyooka, Gerald Cabusao and Thang Nguyen, "Micro channel vapor chamber for high heat spreading", IEEE 2008.
- [7] Prasher R., "A Simplified Conduction Based Modeling Scheme for Design Sensitivity Study of Thermal Solution Utilizing Heat Pipe and Vapor Chamber Technology", J. Electronic Packaging, Vol. 125, pp. 378-385, 2003.
- [8] Wikipedia: https://en.wikipedia.org/wiki/Computational_fluid_dynamics
- [9] ANSYS Icepak User's Guide, Release 15.0, November 2013.
- [10] 6th Generation Intel® Processor Data Sheet for H-Platforms.

Biographical Information

Yasir Aziz Modak, has received her Bachelor of Engineering degree in Mechanical Engineering from the Shivaji University, Maharashtra, India in May 2014. He has completed his Masters in Mechanical Engineering from the University of Texas at Arlington, USA in May 2016. Working with the EMNSPC team he discovered his strong inclination towards CFD, Thermal Sciences and Electronic Packaging area. His research was always dedicated with concise and in depth knowledge of those areas.

After graduation he is ready to get wind of intriguing opportunities down the line of mechanical engineering which would tailor him to become a successful entrepreneur in the field of engineering.